Fluorescence of Amphiphilic Hemicyanine Dyes without Free Double Bonds

Heinz Ephardt and Peter Fromherz*

Abteilung Biophysik der Universität Ulm, D-7900 Ulm-Eselsberg, Germany

Received: November 24, 1992; In Final Form: January 28, 1993

Amphiphilic hemicyanine dyes were obtained by coupling unpolar derivatives of aniline and naphthylamine, respectively, to polar derivatives of pyridinium and isoquinolinium, respectively. These dyes have no free double bond that is prone to photoisomerization. They are effective voltage-sensitive probes in biomembranes. The dyes were characterized by their spectra of absorption and by the spectra, the quantum yields, and the lifetimes of fluorescence. (i) An enhanced polarity of solvents shifts the absorption to the blue and the fluorescence to the red. The solvatochromism is described by an enhancement of the Stokes shift at an invariant 00 energy. (ii) An enhanced polarity lowers the quantum yield of fluorescence by orders of magnitude. The effect is described by an enhancement of nonradiative deactivation at an invariant radiative decay. The enhancements of the Stokes shift and of the nonradiative decay are assigned to two types of intramolecular charge-transfer that couple to polar solvents. The first one is induced by electronic excitation. The second one is induced by intramolecular twist in the excited state. The properties of the dyes in amphiphilic assemblies are discussed in terms of their properties in bulk solvents.

Introduction

Little is known about signal processing within the arborizations of nerve cells. Promising tools to elucidate voltage transients at an adequate spatiotemporal resolution (1 μm, 10 kHz) are membrane-bound fluorescent dyes.[1,2] Usually zwitterionic amphiphilic hemicyanines are used that are derivatives of aminostyrylpyridinium and its homologs with two and three conjugated double bonds.[3,4] A prototype—called di4ASPBS[4] or RH364[5]—is shown in Figure 1 (dye 0).

One drawback of these styryl dyes is their rather low quantum yield of fluorescence. Two effects compete with radiative decay: (i) trans–cis photoisomerism of double bonds;[6] (ii) internal conversion through rotamerism around single bonds.[6-8] We expect to develop improved probes by suppressing photoisomerism and rotamerism.

In the present paper we consider a set of four hemicyanines without free double bond, i.e., without photoisomerism: The electron donors aniline and naphthylamine are attached directly to the electron acceptors pyridinium and isoquinolinium, respectively (Figure 1). In the (aminophenyl)pyridinium (dye 1, BABP) the double bond of (aminostyryl)pyridinium is eliminated.[7] In the (aminonaphthyl)pyridinium (dye 2, BNBP) and in the (aminophenyl)isoquinolinium (dye 3, BABIQ) the double bond of (aminostyryl)pyridinium is bridged. The (aminonaphthyl)-isoquinolinium (dye 4, BNBIQ) may be considered as a derivative of a homologous diphenylbutadiene dye (RH160[4]) with bridged double bonds. In the present paper the solvent-dependent fluorescence of the four dyes is described and rationalized in terms of simple concepts on the interaction of intramolecular charge transfer with the solvent. The study provides a firm basis for the application of the dyes as voltage-sensitive probes in neuron membranes[9] and in lipid bilayers.[10]

Materials and Methods

Synthesis. We obtained the dyes **1–4** (Figure 1) from the corresponding arylpyridines and arylisoquinolines by reaction with butanesultone.[11] 4-[4-(Dibutylamino)phenyl]pyridine and 4-[2-(6-(dibutylamino)naphthalene)]pyridine were prepared by palladium-catalyzed coupling of diethyl(4-pyridyl)borane with *p*-bromo-*N*,*N*-dibutylaniline and with 6-bromo-*N*,*N*-dibutyl-2-naphthylamine according to a procedure for the synthesis of arylpyridines.[12] 6-[4-(Dibutylamino)phenyl]isoquinoline and 6-[2-(6-(dibutylamino)naphthalene)]isoquinoline were prepared by palladium-catalyzed coupling of 6-bromoisoquinoline with the Grignard reagents of *p*-bromo-*N*,*N*-dibutylaniline and of 6-bromo-*N*,*N*-dibutyl-2-naphthylamine according to a procedure for the synthesis of asymmetrical biaryls.[13] (For details see the Appendix.)

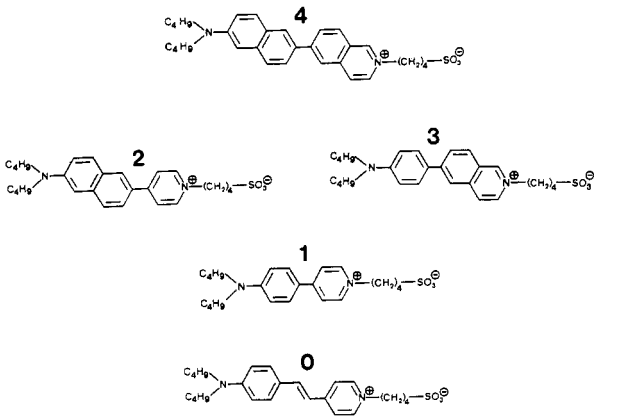

Figure 1. Four amphiphilic hemicyanine dyes without free double bonds. Dye 1 consists of a dibutyl derivative of aniline and a sulfonatobutyl derivative of pyridinium (abbreviation BABP). Dye 2 consists of a dibutyl derivative of naphthylamine and a sulfonatobutyl derivative of pyridinium (BNBP). Dye 3 consists of a dibutyl derivative of aniline and a sulfonatobutyl derivative of isoquinolinium (BABIQ). Dye 4 consists of a dibutyl derivative of naphthylamine and a sulfonatobutyl derivative of isoquinolinium (BNBIQ). For comparison the (aminostyryl)pyridinium dye 0 (di4ASPBS/RH364) is shown at the bottom.

Absorption and Fluorescence. The absorption spectra were measured with a Varian Cary 219 spectrophotometer at 25 °C. Solutions (8.7 μM) of the dye were used as prepared from an 0.87 mM ethanolic stock solution. They contained 1% ethanol. Solvents of highest available purity were used (Merck/Darmstadt and Fluka/Neu-Ulm). Dispersions of sodium dodecyl sulfate (SDS), dodecyltrimethylammonium bromide (DTAB), and egg lecithin were prepared at concentrations of 35 mM, 60 mM, and 1.25 mM, respectively, in water as described in ref 7. Corrected fluorescence emission spectra were recorded at 25 °C by a Spex-Fluorolog fluorometer at excitation wavelengths of 436 nm (dyes 1 and 3) and of 488 nm, respectively (dyes 2 and 4), at a spectral

* Correspondence author.

0022-3654/93/2097-4540$04.00/0

TABLE I: Photophysical Parameters of Dye 1 at 25 °C: Wavenumbers ($\bar{\nu}_A$ and $\bar{\nu}_F$) of the Maxima of Absorption and Fluorescence, Half Widths (HW_A and HW_F) of Absorption and Fluorescence, Decadic Logarithm of the Maximal Decadic Extinction Coefficient ϵ_A (L/(mol cm)), Quantum Yield Φ_F, and Lifetime τ_F of Fluorescence

solvent	$\bar{\nu}_A/(cm^{-1} \times 10^3)$	$HW_A/(cm^{-1} \times 10^3)$	$\log \epsilon_A$	$\bar{\nu}_F/(cm^{-1} \times 10^3)$	$HW_F/(cm^{-1} \times 10^3)$	Φ_F	τ_F/ns
water	23.20	3.31	4.61	18.62	4.00	0.0009	
ethylene glycol	22.94	2.93	4.64	18.98	3.56	0.024	0.15
dimethylformamide	23.26	2.99	4.66	18.74	3.81	0.0045	
acetonitrile	23.20	3.04	4.67	18.42	5.02	0.0019	
methanol	23.04	2.83	4.71	19.00	4.57	0.0026	
ethanol	22.99	2.83	4.73	19.09	4.23	0.0080	
acetone	23.37	3.04	4.64	18.60	4.82	0.0040	
propanol	22.99	2.77	4.68	19.23	4.17	0.016	0.14
cyclopentanol	22.94	2.77	4.68	19.33	3.81	0.067	0.39
butanol	22.99	2.72	4.70	19.26	3.98	0.027	0.19
cyclohexanol	23.10	2.75	4.71	19.41	3.75	0.14	0.75
pentanol	23.10	2.75	4.68	19.32	3.85	0.044	0.27
hexanol	23.15	2.70	4.66	19.44	3.75	0.066	0.37
benzyl alcohol	22.57	2.58	4.66	18.91	3.67	0.071	
octanol	23.20	2.73	4.68	19.52	3.65	0.11	0.59
dichloromethane	22.42	2.49	4.75	18.77	4.10	0.15	1.68
decanol	23.04	2.57	4.67	19.71	3.60	0.17	0.80
chloroform	22.37	2.28	4.78	19.36	3.59	0.26	2.03
SDS	23.15	2.98	4.59	19.30	3.67	0.018	0.12
DTAB	23.42	3.00	4.62	19.52	3.57	0.025	0.17
lecithin	23.36	3.42	4.57	19.57	3.54	0.019	

TABLE II: Photophysical Parameters of Dye 2 at 25 °C: Wavenumbers ($\bar{\nu}_A$ and $\bar{\nu}_F$) of the Maxima of Absorption and Fluorescence, Half Widths (HW_A and HW_F) of Absorption and Fluorescence, Decadic Logarithm of the Maximal Decadic Extinction Coefficient ϵ_A (L/(mol cm)), Quantum Yield Φ_F, and Lifetime τ_F of Fluorescence

solvent	$\bar{\nu}_A/(cm \times 10^3)$	$HW_A/(cm \times 10^3)$	$\log \epsilon_A$	$\bar{\nu}_F/(cm \times 10^3)$	$HW_F/(cm \times 10^3)$	Φ_F	τ_F/ns
water	22.08	4.69	4.29	15.23	2.99	0.0055	
ethylene glycol	21.46	3.90	4.48	15.57	2.78	0.14	0.97
dimethylformamide	21.79	3.94	4.44	15.37	2.79	0.060	0.46
acetonitrile	21.74	3.88	4.45	15.28	2.84	0.025	0.21
methanol	21.51	3.86	4.49	15.47	2.85	0.025	0.21
ethanol	21.46	3.78	4.51	15.60	2.78	0.070	0.48
acetone	21.93	3.89	4.47	15.47	2.84	0.057	0.43
propanol	21.37	3.71	4.50	15.74	2.82	0.13	0.74
cyclopentanol	21.28	3.64	4.50	16.00	2.83	0.37	
butanol	21.37	3.67	4.48	15.78	2.84	0.20	
cyclohexanol	21.41	3.69	4.49	16.02	2.88	0.46	
pentanol	21.41	3.69	4.50	15.88	2.80	0.27	
hexanol	21.44	3.61	4.51	15.95	2.81	0.35	
benzyl alcohol	20.92	3.52	4.50	15.81	2.74	0.39	
octanol	21.55	3.59	4.50	16.12	2.87	0.46	
dichloromethane	20.62	3.33	4.51	16.07	2.60	0.55	3.2
decanol	21.69	3.54	4.46	16.29	2.96	0.51	
chloroform	20.41	3.07	4.53	16.70	2.60	0.65	3.5
SDS	21.83	4.05	3.85	15.81	3.04	0.10	0.80
DTAB	22.12	3.98	4.45	15.69	3.14	0.15	0.80
lecithin	22.78	4.10	4.35	16.07	3.27	0.21	1.8

width of emission of 2.3 nm. Solutions with concentrations of 3–10 μM were used (0.3–1% ethanol). To determine the quantum yields of fluorescence, we used as standards acridine yellow (Aldrich/Steinheim) in ethanol (quantum yield 0.47)[14] for dyes 1 and 3 and rhodamine 6G in ethanol (quantum yield 0.88)[14] for dyes 2 and 4. The calibration was reliable up to 800 nm. Lifetimes down to 0.1 ns were measured at an excitation wavelength of 466 nm and emission wavelengths above 490 nm. A double-cavity dye laser with two stages of amplification was used which was pumped by a terphenyl laser as driven by an excimer laser.[7] The decay kinetics was recorded by a photodiode using a sampling technique. The signal was deconvoluted using a Marquardt algorithm. The residuals were randomly distributed under the assumption of a single exponential with a root mean square deviation <1.3% normalized to the amplitude. Data which deviated distinctly from exponential decay were not considered.

MNDO Computation. To obtain a rough description of the molecular properties in the ground state S_0 and in the first excited singlet state S_1, we computed the energies and the distribution of electric charge by the MNDO model.[15] We applied the program package MOPAC[16] to the chromophores with two methyl groups at the amino nitrogen and one methyl group at the ring nitrogen.[7] We evaluated (i) the optimal dihedral angle ϕ_{opt} between the planes of the two aromatic ring systems in the ground state, (ii) the wavenumber $\bar{\nu}^*$ of the electronic excitation energy at ϕ_{opt}, (iii) the distance Δx^* by which the center of the charge distribution (of an elementary charge e_0) is shifted by excitation along the molecule (parallel to the bond joining the two aromatic moieties), (iv) the fractions α_D and α_D^* of the charge e_0 located in the donor moieties in S_0 and S_1 at ϕ_{OPT}, and (v) the fraction α_D^{90} of the charge e_0 in the donor in S_1 at a twist angle of 90°.

Results and Discussion

At first we describe the spectral properties of the dyes in various bulk solvents. Then we consider the radiative and radiationless deactivation of the first excited singlet state. Finally we discuss the pecularities of the dyes bound to amphiphilic assemblies.

Solvatochromism. The wavenumbers $\bar{\nu}_A$ and $\bar{\nu}_F$ of the maxima of absorption and fluorescence of the dyes 1–4 in 18 solvents are shown in the Tables I–IV. They are plotted in Figure 2 versus the dielectric constant ϵ of the solvents. There is a tendency that the spectra of absorption are shifted to the blue in polar solvents whereas the spectra of fluorescence are shifted to the red. The shifts are almost symmetrical upward and downward. (The logarithmic scale in Figure 2 is used only for convenience.

TABLE III: Photophysical Parameters of Dye 3 at 25 °C: Wavenumbers ($\bar{\nu}_A$ and $\bar{\nu}_F$) of the Maxima of Absorption and Fluorescence, Half Width HW_A of Absorption, Decadic Logarithm of the Maximal Decadic Extinction Coefficient ϵ_A (L/(mol cm)) and Quantum Yield Φ_F of Fluorescence[a]

solvent	$\bar{\nu}_A/(cm^{-1} \times 10^3)$	$HW_A/(cm^{-1} \times 10^3)$	log ϵ_A	$\bar{\nu}_F/(cm^{-1} \times 10^3)$	Φ_F
water	22.94	5.12	3.64	13.0	0.0002
ethylene glycol	22.42	4.38	3.70	13.58	0.002
dimethylformamide	22.78	4.40	3.69	12.6	0.001
acetonitrile	22.78	4.25	3.71	12.9	0.0005
methanol	22.52	4.51	3.74	13.0	0.001
ethanol	22.52	4.05	3.69	13.0	0.002
acetone	22.88	4.42	3.68	12.9	0.001
propanol	22.47	4.26	3.71	13.6	0.002
cyclopentanol	22.37	4.13	3.71	13.4	0.01
butanol	22.52	4.21	3.74	13.8	0.003
cyclohexanol	22.42	4.13	3.72	14.9	0.02
pentanol	22.52	4.21	3.72	14.0	0.004
hexanol	22.52	4.21	3.72	14.1	0.005
benzyl alcohol	22.08	3.91	3.74	14.0	0.005
octanol	22.62	4.30	3.70	14.5	0.01
dichloromethane	21.98	3.95	3.73	14.4	0.01
decanol	22.62	4.25	3.69	14.6	0.01
chloroform	22.03	3.78	3.75	14.5	0.01
SDS	22.37	3.81	3.44	14.3	0.002
DTAB	22.99	4.37	3.68	14.7	0.002
lecithin	23.04	4.77	3.63		

[a] The values of Φ_F are estimated upper limits because of the limited range of calibration of the fluorometer. Half width and lifetime of fluorescence were not determined because of the weak fluorescence. In cyclohexanol a second fluorescence maximum at 19 500 cm^{-1} was observed. In lecithin a maximum of fluorescence could not be determined.

However, it is noteworthy that the spectral shifts are almost linear in that scale).

For each dye the 00 energy $\bar{\nu}_{00} = (\bar{\nu}_A + \bar{\nu}_F)/2$ is almost independent of the environment despite the enormous polarity of the molecules. I.e., the overall stabilization by solvation is similar in the excited state and in the ground state. The 00 energies (Figure 2) are around 21 000, 18 500, 18 100, and 17 100 cm^{-1} for dyes 1, 2, 3, and 4. They drop with the size of the chromophore.

For comparison we computed the excitation energies by the MNDO model. We determined first the optimal geometry in the ground state. (We found that the chromophores are twisted around the single bond between the two aromatic moieties. The dihedral angle ϕ_{opt} (Table V) increases with the size of the chromophore in the series dye 1, 2/3, and 4.) For the optimal geometry we determined the energy difference of electronic excitation $\bar{\nu}^*$ in vacuum (Table V). We obtained $\bar{\nu}^* = 22\,100$, 19 500, 20 000, and 17 800 cm^{-1} for the dyes 1, 2, 3, and 4. These values are surprisingly close to the 00 energies measured in condensed phase.

For each dye the Stokes shift $\bar{\nu}_{ST} = \bar{\nu}_A - \bar{\nu}_F$ is enhanced considerably in polar solvents. Its sensitivity with respect to a change of polarity increases with the size of the chromophore in the series dye 1, dyes 2/3, and dye 4. Yet all Stokes shifts of dye 3 are higher than those of dye 2; e.g. $\bar{\nu}_{ST}$ of dye 3 at the lowest available polarity (chloroform) corresponds to $\bar{\nu}_{ST}$ of dye 2 at the highest available polarity (water) (cf. Figures 2 and 3)! The Stokes shifts of dye 3 are also larger than those of dye 4 in similar solvents.

The opposite shift of absorption and emission spectra cannot be explained by the conventional model of solvatochromism that is based on a point-dipole description of charge distribution.[17-19] Within that approach an opposite shift is expected if the dipole moment is reversed by excitation.[19] However, excitation of dyes 1–4 shifts positive charge from the heteroaryl toward the aminoaryl moiety according to the MNDO calculations (Table V), giving rise to an enhancement of the dipole moments of the zwitterionic molecules. The distance by which the charge is shifted along the chromophores is $\Delta x^* = 0.24$, 0.33, 0.37, and 0.5 nm for dyes 1, 2, 3, and 4. It increases with the size of the chromophore. In the ground states only a fraction of about $\alpha_D = 10\%$ of the charge is localized in the donor moiety whereas in the excited state—at optimal geometry—a fraction of about $\alpha_D^* = 70\%$ is localized in the donor moiety.

The interaction of the solvent with the pattern of charge in the molecule has to be considered in more detail to rationalize the spectral shifts. In a first approximation we assume that the solvation of the sulfonate is independent on the solvation of the chromophore, i.e. that the solvatochromism is a sole property of the positively charged chromophore itself. In the ground state the relaxed solvation shell forms preferentially around the charged pyridinium or isoquinolinium, respectively. In the excited state a similar relaxed solvation shell forms around the charged aniline or aminonaphthalene, respectively. Thus the geometry of the solvation shell differs distinctly in the ground state and in the excited state. This difference increases in polar environments by stronger solvation of the positive moieties of the dye. The argument suggests an enhanced reorganization energy in polar solvents as reflected indeed by the enhanced experimental Stokes shifts. On the other hand the 00 energy is expected to remain unchanged because the solvation energy increases with polarity

TABLE IV: Photophysical Parameters of Dye 4 at 25 °C: Wavenumbers ($\bar{\nu}_A$ and $\bar{\nu}_F$) of the Maxima of Absorption and Fluorescence, Half Widths (HW_A and HW_F) of Absorption and Fluorescence, Decadic Logarithm of the Maximal Decadic Extinction Coefficient ϵ_A (L/(mol cm)), Quantum Yield Φ_F, and Lifetime τ_F of Fluorescence

solvent	$\bar{\nu}_A/(cm^{-1} \times 10^3)$	$HW_A/(cm^{-1} \times 10^3)$	log ϵ_A	$\bar{\nu}_F/(cm^{-1} \times 10^3)$	$HW_F/(cm^{-1} \times 10^3)$	Φ_F	τ_F/ns
water	22.37	6.12	4.18	13.77	3.23	0.002	
ethylene glycol	21.37	4.66	4.37	13.01		0.0049	
dimethylformamide	21.69	4.39	4.38	12.0		0.0017	
acetonitrile	21.74	4.51	4.38	12.0		0.0007	
methanol	21.46	4.58	4.36	12.71		0.0011	
ethanol	21.32	4.49	4.38	12.86	2.92	0.0039	
acetone	21.88	4.51	4.39	12.61		0.0014	
propanol	21.19	4.45	4.40	13.26	3.30	0.0083	
cyclopentanol	20.92	4.10	4.36	13.86	3.76	0.029	0.15
butanol	21.19	4.32	4.35	13.48		0.012	
cyclohexanol	21.19	4.28	4.32	14.24	3.90	0.061	
pentanol	21.14	4.28	4.39	13.67		0.022	0.10
hexanol	21.19	4.24	4.35	13.88	3.78	0.029	0.13
benzyl alcohol	20.62	4.17	4.34	13.28		0.018	0.12
octanol	21.19	4.21	4.40	14.21	3.99	0.058	0.23
dichloromethane	20.45	4.02	4.35	13.35		0.023	
decanol	21.28	4.15	4.41	14.52	3.99	0.10	
chloroform	20.16	3.83	4.36	14.17	3.18	0.17	
SDS	21.51	4.37	3.70	16.29	3.54	0.029	
DTAB	21.83	4.43	4.10	15.43	4.90	0.028	
lecithin	22.62	4.38	4.03	16.09	4.02	0.13	

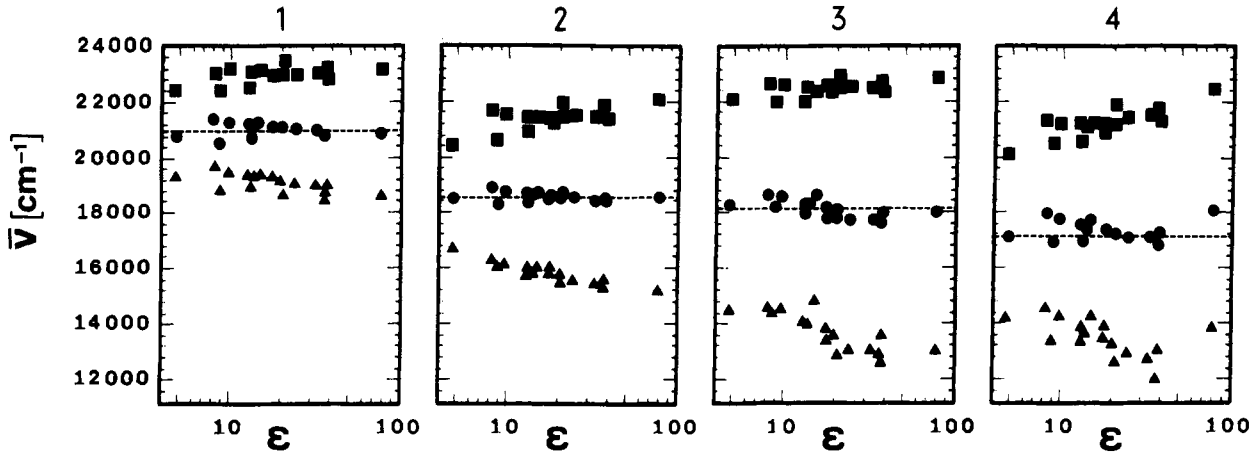

Figure 2. Spectral properties of the dyes 1–4 (from left to right). The wavenumbers of the maxima of absorption $\bar{\nu}_A$ (squares) and fluorescence $\bar{\nu}_F$ (triangles) and of the 00 energy $\bar{\nu}_{00} = (\bar{\nu}_A + \bar{\nu}_F)/2$ (dots) are plotted versus the logarithm of the dielectric constant ϵ of 18 solvents. The dashed lines mark average 00 energies.

TABLE V: Molecular Parameters of Dyes 1–4 As Obtained from Quantum Chemical MNDO Computations for Chromophores with Two Methyl Substituents at the Amino Group and a Methyl Group at the Pyridine/Isoquinoline Nitrogen[a]

parameter	dye 1	dye 2	dye 3	dye 4
optimal dihedral angle φ_{opt}/deg in the ground state	49	57	69	78
excitation energy $\bar{\nu}^*/(\text{cm}^{-1} \times 10^3)$ at φ_{opt}	22.1	19.5	20.0	17.8
charge shift Δx^*/nm by excitation at φ_{opt}	0.24	0.33	0.37	0.50
fraction of elementary charge α_D in the donor (ground state at φ_{opt})	0.16	0.13	0.07	0.07
fraction of elementary charge α_D^* in the donor (excited state at φ_{opt})	0.69	0.71	0.67	0.79
fraction of elementary charge α_D^{90} in the donor (excited state at 90°)	0.90	0.92	0.71	0.87

[a] For details see text.

in ground state as well as in the excited state with their similar—only reversed—localization of charge.

As a heuristic approach we use the Marcus theory for intermolecular charge transfer[20] to describe solvatochromism by intramolecular charge transfer. To the intramolecular (vibrational) reorganization energy $\bar{\nu}_{IM}$ we add the reorganization energy of solvation $\bar{\nu}_{SOLV}$ formulated according to Marcus. We expect a linear relation of the total Stokes shift $\bar{\nu}_{ST} = 2(\bar{\nu}_{IM} + \bar{\nu}_{SOLV})$ and the polarity parameter $n^{-2} - \epsilon^{-1}$ (n refractive index) according to eq 1. β is the fraction of elementary charge that is transferred by excitation, d is the distance of donor and acceptor, r is their radius, and $\alpha_S = 1/137$ is Sommerfeld's fine-structure constant.[20]

$$\bar{\nu}_{ST} = 2\bar{\nu}_{IM} + \frac{\alpha_S \beta^2}{\pi}\left[\frac{1}{r} - \frac{1}{d}\right]\left[\frac{1}{n^2} - \frac{1}{\epsilon}\right] \qquad (1)$$

On the basis of eq 1 we plot the experimental Stokes shifts versus $n^{-2} - \epsilon^{-1}$ (Figure 3). The data may be interpolated by straight lines indeed. We evaluate the slopes $\Delta\bar{\nu}_{ST}/\Delta(n^{-2} - \epsilon^{-1})$ = 4500, 8300, 8300, and 13300 cm^{-1} for dyes 1, 2, 3, and 4. To check the model for consistency, we may compute the radius r, inserting for the fraction of charge β and for the distance d values from the MNDO calculation (cf. Table V) with $\beta = \alpha_D^* - \alpha_D$, the change of charge in the donor, and with $d = \Delta x^*$, the displacement of charge by excitation. We obtain the radii r = 0.21, 0.24, 0.27, and 0.32 nm for dyes 1–4. These values are in a reasonable order of magnitude.

The intramolecular part of the reorganization energy is obtained by extrapolating $\bar{\nu}_{ST}$ to $n^{-2} - \epsilon^{-1} = 0$. From Figure 3 we obtain $\bar{\nu}_{IM}$ = 1000 cm^{-1} for dyes 1, 2, and 4 but $\bar{\nu}_{IM}$ = 2500 cm^{-1} for dye 3. We have no explanation for this striking exception of dye 3.

Strength of Absorption. The extinction coefficient ϵ_A at the maximum of absorption $\bar{\nu}_A$ and the half widths HW_A of the absorption spectra in 18 solvents are shown in the Tables I–IV for dyes 1–4. From ϵ_A and HW_A we evaluate the transition dipole moment of excitation d_{EX} according to eq 2[21] using the approximation $\int d\bar{\nu}_A(\epsilon_A/\bar{\nu}_A) = \epsilon_A HW_A/\bar{\nu}_A$.

$$\left[\frac{d_{EX}}{e_0}\right]^2 = \frac{3}{4\pi^2\alpha_S}\frac{(\ln 10)\,\epsilon_A\,HW_A}{n\bar{\nu}_A} \qquad (2)$$

The parameter $\epsilon_A HW_A/n\bar{\nu}_A$ is plotted in Figure 4 versus the dielectric constant ϵ. It is rather invariant for each dye. The transition dipoles in ethanol are d_{EX} = 5.3, 5.2, 2.0, and 4.9 D for dyes 1–4. Surprisingly d_{EX} decreases with increasing size of the chromophore in the series dyes 1, 2, and 4; this drop may be due to the enhanced twist of the two aromatic systems (cf. Table V). We have no explanation for the low transition moment of dye 3.

Quantum Yield of Fluorescence. The quantum yields Φ_F of fluorescence of dyes 1–4 in 18 solvents are shown in Tables I–IV and plotted in Figure 5 versus the dielectric constant ϵ. For all four dyes there is a trend that polar solvents lower the quantum yield by more than 2 orders of magnitude. The quantum yield Φ_F is proportional to the lifetime τ_F of fluorescence for dyes 1, 2, and 4 (Tables I, II, and IV) as illustrated in Figure 6. I.e., the rate constants of radiative decay k_F evaluated from $\Phi_F = k_F\tau_F$ are rather invariant. Thus we assign the modulation of Φ_F to a modulation of radiationless deactivation i.e. of a rate constant k_I of some pathway of internal conversion according to the relation $\Phi_F = k_F/(k_F + k_I)$.

Radiative Deactivation. Average rate constants of radiative decay are evaluated from quantum yield and lifetime of fluorescence using $\Phi_F = k_F\tau_F$. We obtain for dyes 1, 2, and 4 k_F = 0.16, 0.16, and 0.2 ns^{-1}, respectively. For comparison we compute k_F from the spectra of absorption and emission. k_F depends on the transition dipole moment of emission d_{EM} and on the wavenumber $\bar{\nu}_F$ of the fluorescence maximum according to eq 3.[21] The approximation $\int d\bar{\nu}\, f_{\bar{\nu}}/\bar{\nu}^3 = \bar{\nu}_F^{-3}$ is used to evaluate the normalized fluorescence spectrum $f_{\bar{\nu}}$. (c is the velocity of light.)

$$k_F = \frac{4\pi^2\alpha_S}{3}\,8\pi c(n\bar{\nu}_F)^3\left[\frac{d_{EM}}{e_0}\right]^2 \qquad (3)$$

If the transition dipole moments of emission and excitation are equal as $d_{EM} = d_{EX}$, we may substitute $(d_{EM}/e_0)^2$ as given by eq 2 to obtain the well-known relation of Strickler and Berg.[22] We compute k_F = 0.26, 0.12, and 0.06 ns^{-1} for dyes 1, 2, and 4 in ethanol. These values are not too far from those obtained from quantum yield and lifetime of fluorescence. However, the systematic decrease of k_F with the length of the chromophore is not visible there. For dye 3 we compute an extremely slow rate

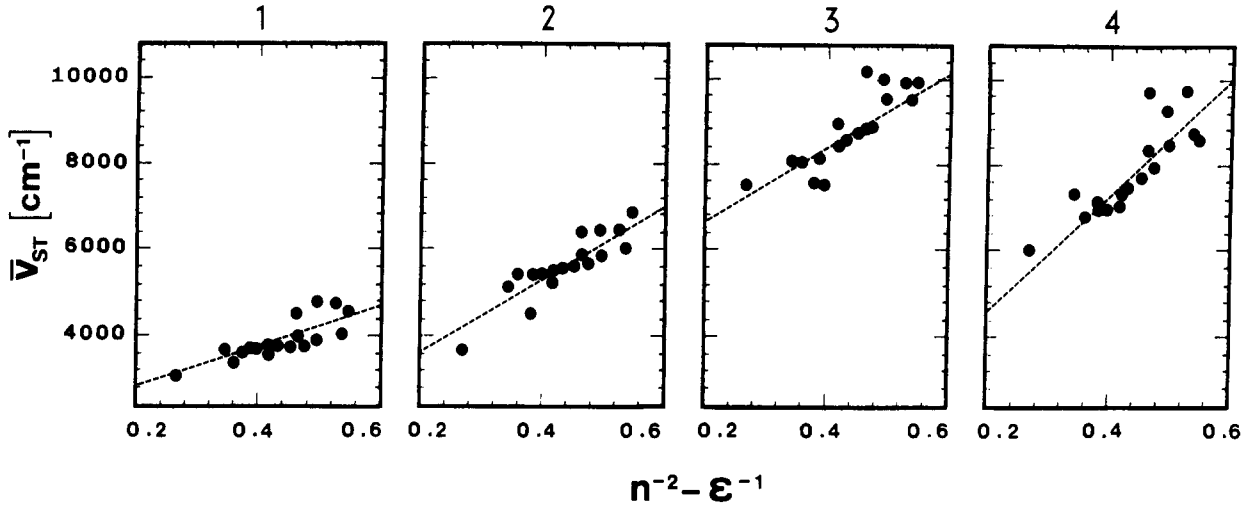

Figure 3. Stokes shift $\bar{\nu}_{ST} = \bar{\nu}_A - \bar{\nu}_F$ of the dyes 1–4 (from left to right) versus the polarity parameter $n^{-2} - \epsilon^{-1}$, the difference of the reciprocal square of refractive index n, and of the reciprocal dielectric constant ϵ. The slopes of the lines are 4500, 8300, 8300, and 13300 cm^{-1}. Their intersections are 1000, 1000, 2500, and 1000 cm^{-1}.

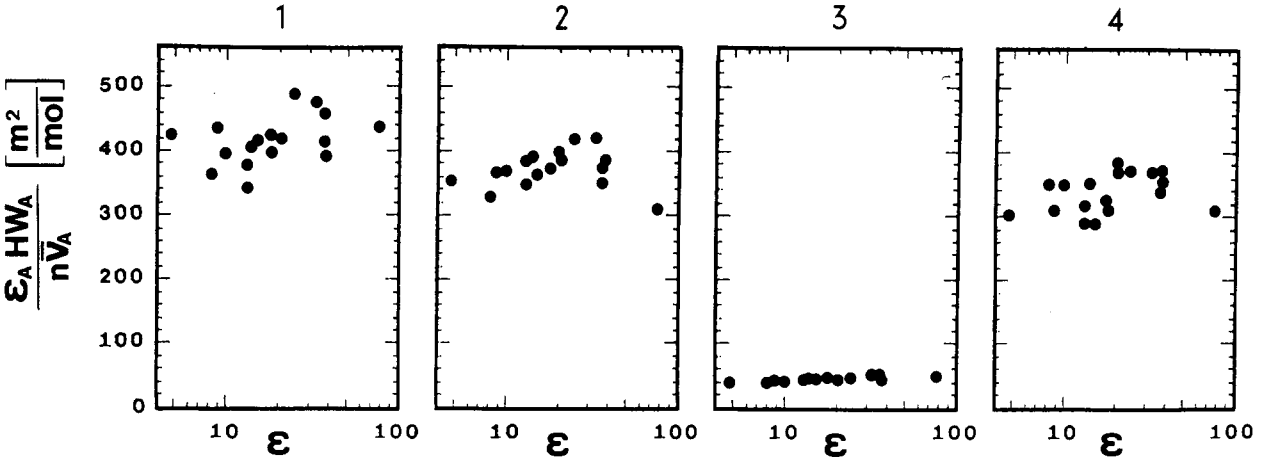

Figure 4. Strength of absorption of the dyes 1–4 expressed by the term $\epsilon_A HW_A/n\bar{\nu}_A$ (maximal extinction coefficient ϵ_A, half width of absorption spectrum HW_A, wavenumber of maximal absorption $\bar{\nu}_A$, and refractive index n) versus the logarithm of the dielectric constant ϵ of 18 solvents.

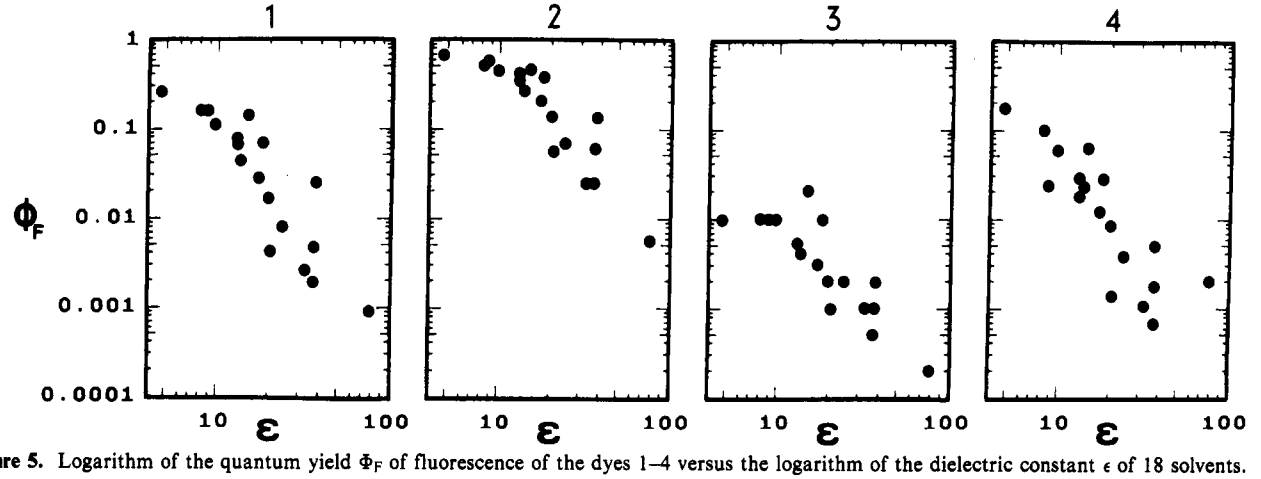

Figure 5. Logarithm of the quantum yield Φ_F of fluorescence of the dyes 1–4 versus the logarithm of the dielectric constant ϵ of 18 solvents.

constant, k_F = 0.01 ns^{-1}. This slow radiative decay may be responsible for the low quantum yield of fluorescence of dye 3.

Radiationless Deactivation. We evaluate rate constants of internal conversion for dyes 1, 2, and 4 from $k_I = k_F(\Phi_F^{-1} - 1)$. They change by almost 3 orders of magnitude by changing the solvent. Considering pairs of solvents with similar dielectric constant, we find that the rate constant is always lower in the solvent of higher viscosity. For dyes 1, 2, and 4 we find, e.g., in acetonitrile/ethylene glycol rate constants k_I = 84/6.5 ns^{-1}, k_I = 5.9/0.92 ns^{-1}, and k_I = 300/43 ns^{-1}.

The effect of viscosity per se indicates that an intramolecular motion is involved. As an enhanced viscosity lowers the rate of radiationless deactivation, we must assume that the molecular state that is reached exhibits an enhanced rate of internal conversion. As radiationless deactivation is enhanced in polar solvents, we must assume that the polarity of the molecule is enhanced in the course of that intramolecular reaction.

The MNDO computation indicates that electronic charge is accumulated in the aminoaryl moieties by intramolecular twist in the excited state as indicated (Table V). A fraction of about

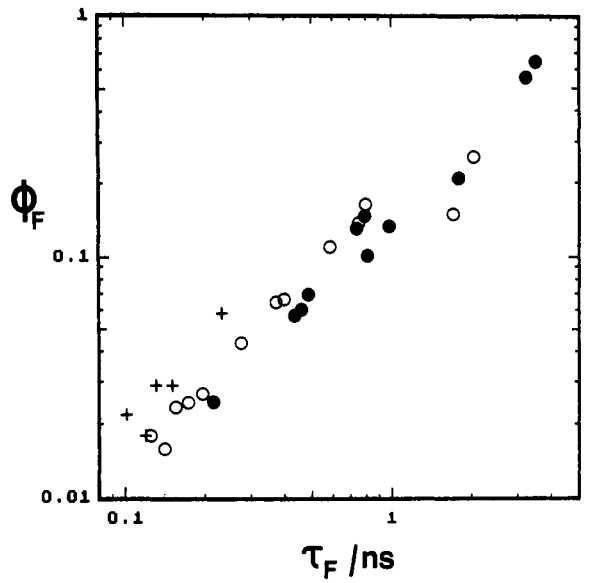

Figure 6. Logarithm of the quantum yield Φ_F of fluorescence versus logarithm of the lifetime τ_F of fluorescence for dye 1 (circles), dye 2 (dots), and dye 4 (crosses).

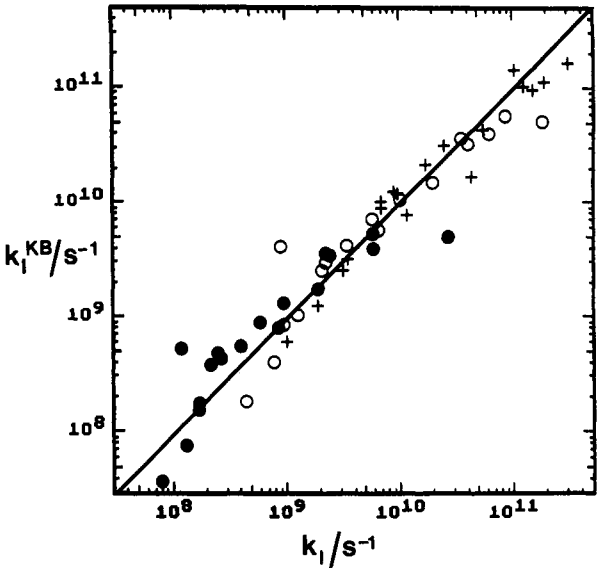

Figure 7. Logarithm of the rate constant k_I^{KB} computed from the Kramers–Born model describing the effects of solvation and friction versus logarithm of the rate constant k_I of internal conversion of dye 1 (circles), dye 2 (dots), and dye 4 (crosses).

$\alpha_D^* = 70\%$ is localized in the donor moiety in the excited state at optimal geometry of the ground state, whereas a fraction of about $\alpha_D^{90} = 90\%$ is localized in the donor if the dihedral angle is enhanced up to 90°. Considering this correlation of intramolecular motion and enhancement of polarity, we assign the intramolecular reaction from a fluorescent to an nonfluorescent state (with fast internal conversion) to an enhancement of twist of the single bond between the two aromatic moieties.[6,7]

The intramolecular reaction cannot be assigned to a planarization of the molecules, which are twisted in their excited state after a Franck-Condon transition; we have shown recently that such a planar molecule—a fluorene derivative of dye 1—has an extremely high yield of fluorescence.[8] Also a rotation of the amino group is unlikely; planarization of an amino group in dye 0 by two six-membered bridges had no significant effect on fluorescence (Ephardt and Fromherz, unpublished observation).

To rationalize the data of radiationless deactivation, we try to describe the rate constant k_I on the basis of Kramers' theory that accounts for an activation energy and for friction.[23] We describe the stabilization of a polar transition state in polar solvents by a Born energy[24] assuming adiabatic relaxation of the solvation shell during the reaction. We obtain eq 4.[6] $\eta_0 = 1$ cP is a standard viscosity, a accounts for deviations from Stokes law, and E^*_{IM} is the intramolecular activation energy.

$$k_I^{KB} = k_I^0 \exp(-E^*_{IM}/RT)(\eta_0/\eta)^a \exp(-E^*_0/\epsilon RT) \quad (4)$$

To document the quality of the fit of the data by eq 4, we plot the fitted rate constants k_I^{KB} versus the experimental data $k_I = k_F(\Phi^{-1} - 1)$ in Figure 7. The fit parameters for dyes 1, 2, and 4 are $a = 0.6$, 0.5, and 0.6, $b = E^*_0/RT = 30$, 26, and 29, and $c = k_I^0 \exp(-E^*_{IM}/RT) = 72$, 6.3, and 220 ns^{-1}. The similarity of the various a parameters and of the various b parameters—that account for the effects of viscosity and polarity—indicates that the same kind of solvent–dye interaction determines radiationless deactivation in dyes 1, 2, and 4. The different values of parameter c indicate different intramolecular properties of the three dyes.

Amphiphilic Assemblies. In lecithin the absorption of all dyes is found at a rather high wavenumber—like in a polar solvent (Tables I–IV). The fluorescence is found at a rather high wavenumber as well—like in an unpolar solvent (Tables I–IV). The spectral shifts in DTAB and SDS are similar. Apparently a rationalization of solvation in amphiphilic assemblies in terms of the property of a bulk solvent—an equivalent polarity—is not possible.

Due to their amphiphilic character, the dyes are presumably bound close to the surface of the lipid bilayer or of the surfactant micelles, i.e. in a region of strong variation of local polarity. We may describe the environment—up to first order—by a local polarity and by a gradient of polarity.

In bulk solvents the 00 energy depends little on polarity (Figure 2). Thus we take the shift of the 00 energy in amphiphilic assemblies as an indicator for the gradient of polarity.

In all cases we observe a blue shift of the 00 energy. E.g., in lecithin we evaluate for dye 1 a shift by 600 cm^{-1}, for dye 2 a shift by 900 cm^{-1}, and for dye 4 a shift by 2300 cm^{-1} as seen from Tables I–IV. We may imagine that unpolar substituents align the chromophore along the gradient of polarity such that the aniline and naphthylamine, respectively, are drawn into an unpolar environment, whereas the pyridinium and isoquinolinium, respectively, stay in a polar environment. Electronic excitation shifts electric charge from an polar to an unpolar environment, such that the stabilization energy of the excited state by solvation is reduced.[25] The enhancement of the blue shift with enhanced size of the chromophore may be due to the enhanced charge shift (cf. Table V) or to a better alignment of the extended chromophores along the gradient of polarity.

The Stokes shift is modulated by the polarity itself in bulk solvents. We may try to use its value in amphiphilic assemblies as an indicator for the local polarity at the site of the dye. For lecithin we evaluate for dyes 1, 2, and 4 $\bar{\nu}_{ST} = 3790$, 6710, and 6530 cm^{-1}. Interpolating these values in Figure 3 we would obtain quite different local polarities for the environment of the three dyes. We see no straightforward physical argument for such different binding sites of the dyes in lecithin.

Conclusions

The fluorescence of the hemicyanine dyes 1–4 is most sensitive with respect to changes of the environment: The solvents give rise to a shift of the spectra of absorption and fluorescence to the blue and to the red, respectively, and to a drop of the quantum yield of fluorescence. The effects may be assigned to intramolecular charge transfer in the processes of excitation and of twist in the excited state and to the interaction of these charge shifts with the environment. The solvatochromism is described by the Marcus model of intermolecular electron transfer. The change of yield is described by the Kramers equation in conjunction with the concept of the Born energy.

The hemicyanine dyes 1–4 have been applied successfully as voltage-sensitive probes in neuron membranes[9] and lipid bilayers.[10] The spectral features of voltage sensitivity differ qualitatively for a given dye, e.g. BNBIQ, in a neuron membrane and in a lipid bilayer and for two similar dyes, e.g. BNBP and BNBIQ, in the neuron membrane. The features of the sensitivity of fluorescence with respect to solvation, as presented in the present paper, are the basis for an assignment of a physical mechanism to the voltage-sensitive fluorescence and for progress in the development of improved probes.

Appendix

Synthesis of Dyes 1–4. Dyes 1–4 were characterized by their melting points taken on a Mettler FP-5 melting point apparatus equipped with a heating desk FP-52, by their mass spectrum measured with a Varian MAT 711 spectrometer (the m/e values of the M peaks are given) and by their ^{1}H NMR spectra measured with a Bruker MSL-300 spectrometer (the chemical shifts (δ values) are given in ppm relative to TMS as a standard). None of the synthesis was optimized for maximum yield.

1-(Sulfonatobutyl)-4-[4-(dibutylamino)phenyl]pyridinium (Dye 1). A 420-mg portion of 4-[4-(dibutylamino)phenyl]pyridine was stirred with 3 mL of 1,4-butanesultone (15-fold molar excess) (Fluka, Neu-Ulm) for 2 h at 130 °C.[11] The product was purified by column chromatography (silica gel 60, Merck) (elution of the impurities with ethanol of the product with methanol) and by recrystallization from ethanol: yield, 140 mg (22%) of yellow crystals; melting point, above 300 °C; ^{1}H NMR (CD_3OD) δ 1.00 (t, J = 7.3 Hz, 6 H), 1.41 (m, 4 H), 1.62 (m, 4 H), 1.83 (m, 2 H), 2.14 (m, 2 H), 2.88 (t, J = 7.3 Hz, 2 H), 3.44 (t, J = 7.6 Hz, 4 H), 4.47 (t, J = 7.3 Hz, 2 H), 6.83 (d, J = 9.2 Hz, 2 H), 7.91 (d, J = 9.2 Hz, 2 H), 8.15 (d, J = 7.2 Hz, 2 H), 8.59 (d, J = 7.1 Hz, 2 H).

1-(Sulfonatobutyl)-4-[2-(6-(dibutylamino)naphthyl)]pyridinium (Dye 2). From reaction of 450 mg of 4-(N,N-dibutyl-2-naphthylamino)pyridine and 3 mL of 1,4-butanesultone, dye 2 was obtained as described above. Purification was by column chromatography (elution with ethanol) and recrystallization from ethanol: yield, 360 mg (55%) orange-red powder; melting point, above 300 °C; ^{1}H NMR (CD_3OD) δ 1.00 (t, J = 7.3 Hz, 6 H), 1.44 (m, 4 H), 1.66 (m, 4 H), 1.86 (m, 2 H), 2.19 (m, 2 H), 2.89 (t, J = 7.3 Hz, 2 H), 3.47 (t, J = 7.6 Hz, 4 H), 4.56 (t, J = 7.4 Hz, 2 H), 6.88 (s, 1 H), 7.20 (d, J = 8.5 Hz, 1 H), 7.74 (d, J = 8.7 Hz, 1 H) 7.83–7.87 (m, 2 H), 8.38–8.40 (m, H), 8.79 (d, J = 7.0 Hz, 2 H).

2-(Sulfonatobutyl)-6-[4-(dibutylamino)phenyl]isoquinolinium (Dye 3). From reaction of 360 mg of 6-[4-(dibutylamino)phenyl]-isoquinoline and 2.3 mL of 1,4-butanesultone, dye 3 was obtained, after recrystallization from ethyl acetate/ethanol (10:1): yield, 143 mg (28%) of yellow powder; melting point, 223.5–225 °C; ^{1}H NMR (CD_3OD) δ 1.01 (t, J = 7.3 Hz, 6 H), 1.44 (m, 4 H), 1.62–1.73 (m, 6 H), 2.10 (m, 2 H), 2.73 (t, J = 7.4 Hz, 2 H), 3.46 (t, J = 7.7 Hz, 4 H), 4.60 (t, 2 H), 6.96 (d, J = 9.0 Hz, 2 H), 7.40 (d, J = 8.9 Hz, 2 H), 7.89–7.93 (m, 2 H), 8.12–8.18 (m, 1 H), 8.28 (d, J = 8.2 Hz, 1 H), 8.41 (d, J = 7.0 Hz, 1 H), 8.72 (d, J = 7.0 Hz, 1 H).

2-(Sulfonatobutyl)-6-[2-(6-(dibutylamino)naphthyl)]isoquinolinium (Dye 4). From reaction of 1 g of 6-[2-(6-N,N-dibutylamino)naphthalene]isoquinoline and 6 mL of 1,4-butanesultone, dye 4 was obtained, after purification by two recrystallizations from ethanol and methanol, respectively: yield, 200 mg (15%) orange platelets; melting point, 288–290 °C; ^{1}H NMR (CD_3OD) δ 1.01 (t, J = 7.0 Hz, 6 H), 1.42 (m, 4 H), 1.66 (m, 4 H), 1.88 (m, 2 H), 2.28 (m, 2 H), 2.91 (t, J = 7.2 Hz, 2 H), 3.47 (t, J = 7.5 Hz, 4 H), 4.74 (t, J = 7.4 Hz, 2 H), 6.90 (s, 1 H), 7.20 (d, J = 9.3 Hz, 1 H), 7.74–7.90 (m, 3 H), 8.26 (s, 1 H), 8.42–8.60 (m, 5 H), 9.77 (s, 1 H).

4-[4-(Dibutylamino)phenyl]pyridine and 4-[2-(6-(Dibutylamino)naphthyl)]pyridine. These products were obtained by reaction of p-bromo-N,N-dibutylaniline and 6-bromo-N,N-dibutyl-2-naphthylamine with diethyl(4-pyridyl)borane under argon atmosphere according to a procedure described by Ishikura.[12] KOH (Merck, Darmstadt), Bu_4NBr (Aldrich), $Pd(Ph_3P)_4$ (Aldrich), and dry THF (Aldrich) were used as received. The products were purified by column chromatography (silica gel 60, n-Hexane/ethyl acetate (2:1)). From 2.3 g of p-bromo-N,N-dibutylaniline (reaction time 18 h), we obtained 500 mg (33%) of 4-[4-dibutylamino)phenyl]pyridine as a yellow oil: MS, m/e = 282 (M^+). From 1.5 g of 6-bromo-N,N-dibutyl-2-naphthylamine (reaction time 7 h), we obtained 450 mg (42%) of 4-[2-(6-(dibutylamino)naphthalene)]pyridine as an orange-yellow oily product: MS, m/e = 332 (M^+).

6-[4-(Dibutylamino)phenyl]isoquinoline. This compound was obtained by a synthesis according to a general procedure described by Widdowson and Zhang.[13] From 9.9 g of p-bromo-N,N-dibutylaniline and 1 g of magnesium we prepared the Grignard reagent in dry THF (initiation by 500 μL ethyl iodide). The reaction was completed by 45 min of refluxing. Coupling reaction: Under an argon atmosphere 600 mg of $Pd(Ph_3P)_4$ was added to 5 g of 6-bromoisoquinoline in 25 mL of dry THF. The freshly prepared Grignard solution was added to the reaction mixture under reflux by use of a syringe. The reaction was completed by 1 h of refluxing. THF was removed under reduced pressure. The product was isolated from the resulting dark red oil by column chromatography (silica gel 60, n-hexane/ethyl acetate (9:1)). A 360-mg amount (4.5%) of oily orange red product was obtained: MS, m/e = 332 (M^+).

6-[2-(6-(Dibutylamino)naphthyl)]isoquinoline. From 6 g of 2-(dibutylamino)-6-bromonaphthalene and 600 mg of magnesium, we prepared the Grignard reagent in 15 mL of THF (initiation by 200 μL of ethyl iodide). Coupling reaction: 3.7 g of 6-bromoisoquinoline in 22 mL of THF and 480 mg of $Pd(Ph_3P)_4$ were used. After removing THF, 200 mL of ether and 200 mL of 1 N hydrochloric acid were added. The ether layer was extracted 3 times with 50 mL of 1 N HCl. The combined aqueous solutions were made alkaline with NaOH and extracted with ether. After evaporation of the ether under reduced pressure, the residual solid was recrystallized from methanol: yield, 2.3 g (33%) of pale yellow platelets; melting point, 148–150 °C; MS, m/e = 382 (M^+).

Diethyl(4-pyridyl)borane. This product was obtained from 4-bromopyridine (freshly prepared from 4-bromopyridine hydrochloride[26,27]) BuLi (1.6 M in hexane, Aldrich), and diethylmethoxyborane according to a procedure described by Ishikura et al.[12] The required diethylmethoxyborane was synthesized[28] in 80% yield from triethylborane (Aldrich) and dry methanol in the presence of diethylboryl pivalate, which was prepared[29] from pivalic acid and triethylborane in n-pentane.

6-Bromoisoquinoline. This product was obtained by reaction of dimethyl(p-bromobenzylidene)aminoacetal, ethyl chloroformate (Aldrich), and trimethyl phosphite (Aldrich) according to a general procedure for the synthesis of substituted isoquinolines[30] in 4% yield after purification by column chromatography (silica gel, chloroform): melting point, 43–44 °C; MS, m/e = 207 (M). The required dimethyl(p-bromobenzylidene)aminoacetal was prepared[31] with bromobenzaldehyde (Aldrich) in 96% yield.

***p*-Bromo-*N*,*N*-dibutylaniline and 6-Bromo-2-(*N*,*N*-dibutylnaphthylamine).** From reaction of 1-butyliodide with 4-bromoaniline (Aldrich) and 6-bromo-2-naphthylamine, respectively, in the presence of potassium carbonate in dry DMF.[11] The products were purified by column chromatography (silica gel 60, n-hexane): p-bromo-N,N-dibutylaniline, 71% yield, MS m/e = 283 (M^+); 6-bromo-2-(N,N-dibutylnaphthylamine), 70% yield, MS m/e = 333 (M^+). The 6-bromo-2-naphthylamine was prepared by Bucherer reaction[32,33] from 6-bromo-2-naphthol (Aldrich) and ammonium sulfite/aqueous ammonia in an autoclave at 150 °C: melting point, 127–128 °C; MS, m/e = 221 (M^+).

Acknowledgment. We thank Karola Kemper and Uwe Theilen for their excellent technical assistance, Dr. Georg Reinbold for help in measuring the fluorescence lifetimes, and Andrea Heilemann for careful reading of the manuscript. We acknowledge the generous support by the Deutsche Forschungsgemeinschaft (Grants Fr 349/4 and Fr 349/5) and by the Fonds der Chemischen Industrie.

References and Notes

(1) Cohen, L. B.; Lesher, S. In *Optical Methods in Cell Physiology*; deWeer, P., Salzberg, B. M., Eds.; Wiley: New York, 1986; p 71.
(2) Fromherz, P.; Dambacher, K. H.; Ephardt, H.; Lambacher, A.; Müller, C. O.; Neigl, R.; Schaden, H.; Schenk, O.; Vetter, T. *Ber. Bunsen-ges. Phys. Chem.* **1991**, *95*, 1333.
(3) Loew, L. M.; Simpson, L. L. *Biophys. J.* **1981**, *34*, 353.
(4) Grinvald, A.; Hildesheim, R.; Farber, I. D.; Anglister, L. *Biophys. J.* **1982**, *39*, 301.
(5) Fluhler, E.; Burnham, V. G.; Loew, L. M. *Biochemistry* **1985**, *24*, 5749.
(6) Ephardt, H.; Fromherz, P. *J. Phys. Chem.* **1989**, *93*, 7717.
(7) Ephardt, H.; Fromherz, P. *J. Phys. Chem.* **1991**, *95*, 6792.
(8) Fromherz, P.; Heilemann, A. *J. Phys. Chem.* **1992**, *96*, 6864.
(9) Fromherz, P.; Müller, C. O. Submitted for publication in *Biochim. Biophys. Acta*.
(10) Fromherz, P.; Schenk, O. Manuscript in preparation.
(11) Hassner, A.; Birnbaum, D.; Loew, L. M. *J. Org. Chem.* **1984**, *49*, 2546.
(12) Ishikura, M.; Ohta, T.; Terashima, M. *Chem. Pharm. Bull.* **1985**, *33*, 4755.
(13) Widdowson, D. A.; Zhang, Y. Z. *Tetrahedron* **1986**, *42*, 2111.
(14) Olmsted, J., III. *J. Phys. Chem.* **1979**, *83*, 2581.
(15) Dewar, M. J. S.; Thiel, W. *J. Am. Chem. Soc.* **1977**, *99*, 4899.
(16) Stewart, J. J. P. *MOPAC Manual*, 2nd ed.; University of Texas, Austin (QCPE, program No. 455).
(17) Onsager, L. *J. Am. Chem. Soc.* **1936**, *58*, 1486.
(18) Ooshika, Y. *Phys. Soc. Jpn.* **1954**, *9*, 594.
(19) Liptay, W. *Z. Naturforsch.* **1965**, *20a*, 144.
(20) Marcus, R. A. *Discuss. Faraday Soc.* **1960**, *29*, 21.
(21) Birks, J. B. *Photophysics of Aromatic Molecules*; Wiley-Interscience: London, 1970.
(22) Strickler, S. J.; Berg, R. A. *J. Chem. Phys.* **1962**, *37*, 814.
(23) Kramers, H. A. *Physica* **1940**, *7*, 284.
(24) Born, M. *Z. Phys.* **1920**, *1*, 45.
(25) Loew, L. M.; Simpson, L.; Hassner, A.; Alexanian, V. *J. Am. Chem. Soc.* **1979**, *101*, 5439.
(26) Gaus, P. L.; Haim, A.; Johnson, F. *J. Org. Chem.* **1977**, *42*, 564.
(27) Desbene, P. L.; Jehanno, N. *J. Heterocycl. Chem.* **1984**, *21*, 1321.
(28) Köster, R.; Fenzl, W.; Seidel, G. *Liebigs Ann. Chem.* **1975**, 352.
(29) Köster, R.; Bellut, H.; Fenzl, W. *Liebigs Ann. Chem.* **1974**, 54.
(30) Hendrickson, J. B.; Rodriguez, C. *J. Org. Chem.* **1983**, *8*, 3344.
(31) Tyson, F. T. *J. Am. Chem. Soc.* **1939**, *61*, 183.
(32) Anderson, L. C.; Johnston, D. *J. Am. Chem. Soc.* **1943**, *65*, 239.
(33) Newman, M. S.; Galt, R. H. B. *J. Org. Chem.* **1960**, *25*, 214.